Integrated Dark Fermentation and Anaerobic Digestion of Organic Waste for Biohydrogen and Biomethane Production: Experimental Validation and Process Simulation

Mehran Ahmadi[a], Ludovico Linzi[b] and Anna Stoppato[c]

[a] University of Padova, Padova, Italy, mehran.ahmadi@studenti.unipd.it
*[b] University of Padova, Padova, Italy, ludovico.linzi@unipd.it, **CA***
[c] University of Padova, Padova, Italy, anna.stoppato@unipd.it

Abstract:

This study investigates an integrated process for the co-conversion of food waste (FW) and waste activated sludge (WAS) into biohydrogen and biomethane through the sequential application of dark fermentation (DF) and anaerobic digestion (AD). The overall system is developed and simulated in Aspen Plus and validated against experimental data. Two feedstock configurations are considered, including a combined mixture (Mix A+B) and an alternative composition (Mix C) with a higher fraction of readily fermentable substrates. In the DF stage, fermentable compounds are converted into hydrogen and volatile fatty acids (VFAs) under mesophilic conditions in a semi-continuous reactor, with hydrogen production rates of 0.79-0.80 $\mathrm{NL(H2)/(L \cdot d)}$, within the reported experimental range. A slightly higher hydrogen production is observed for Mix C, attributed to its increased glucose content and enhanced substrate availability. The liquid effluent from DF is subsequently treated in a thermophilic AD reactor, where residual intermediates are converted into methane, achieving methane production rates of 54.18-58.24 $\mathrm{L/h}$ and specific methane yields of 123.47-124.44 $\mathrm{L/kg_{COD}}$, indicating effective conversion of fermentation products. A moderate increase in methane generation is observed for Mix C, reflecting the higher availability of fermentation-derived intermediates. Overall, the validated model demonstrates the technical feasibility of the integrated DF-AD configuration and its capability to enhance energy recovery from waste streams. The produced biogas streams are suitable for utilisation in solid oxide fuel cells (SOFCs) for high-efficiency electricity generation, and the developed simulation framework provides a reliable tool for process analysis and optimisation, supporting the design and scale-up of integrated waste-to-energy systems.

Keywords: Anaerobic Digestion; Aspen Plus; Biohydrogen; Dark Fermentation; Waste-to-Energy.

1. Introduction

The global community faces a dual energy challenge: the progressive depletion of fossil fuel reserves and the environmental degradation caused by greenhouse gas emissions. Addressing these challenges requires a transition toward sustainable energy systems and a significant reduction in dependence on conventional fossil fuels. Hydrogen ($\mathrm{H_2}$) is a critical component of this transition due to its high energy density and carbon-free combustion profile [1, 2]. Among the various production methods available, biological pathways such as dark fermentation (DF) offer a promising route for the valorization of organic waste streams into clean energy carriers [3].

Dark fermentation (DF) is a key biological pathway for hydrogen production, where anaerobic microorganisms, particularly Clostridium species, convert carbohydrate-rich substrates into hydrogen mainly via acetate- and butyrate-type pathways [3]. Its operational simplicity, independence from light, and ability to process diverse organic waste streams make it a promising technology for waste-to-energy applications.

Food waste and waste activated sludge (WAS) are two important substrates for dark fermentation-based hydrogen production. Food waste is rich in readily fermentable carbohydrates, particularly monosaccharides,

which support rapid microbial activity and high hydrogen yields. In contrast, WAS is a protein-rich residue from wastewater treatment, characterized by high nitrogen content and lower biodegradability due to its complex microbial structure [4]. While each substrate presents limitations when used alone, their co-digestion offers a synergistic approach by improving nutrient balance, diluting inhibitors, and optimizing the $\mathrm{C/N}$ ratio for enhanced fermentation performance.

A key limitation of dark fermentation is its low energy recovery efficiency, as only a fraction of the substrate energy is converted into hydrogen, while a significant portion remains in the form of volatile fatty acids (VFAs) [5]. Discarding these intermediates reduces overall process viability. This limitation can be addressed by integrating dark fermentation with anaerobic digestion (AD), where the VFA-rich effluent is further converted into methane under methanogenic conditions. This DF-AD cascade enables recovery of both hydrogen and biomethane from the same feedstock, improving overall energy yield and enhancing substrate utilization.

The complexity of integrated DF-AD systems, involving multiple biochemical pathways, hydrogen inhibition, and coupled reaction networks, limits the ability of experimental studies alone to fully describe system behavior. Process simulation using tools such as Aspen Plus provides a complementary approach by enabling mechanistic modeling and prediction of system performance. The integration of validated simulation with experimental data is therefore essential for process understanding, optimization, and scale-up of biofuel production systems [6].

A key challenge in the development of biological waste-to-energy systems is the lack of integrated and experimentally validated modeling frameworks capable of accurately representing both hydrogen and methane production pathways. Existing studies have typically focused on individual process stages or simplified models, limiting their applicability for system-level analysis and optimization. Therefore, there is a need for a unified simulation framework that can reliably reproduce experimental behavior while enabling further process evaluation and scale-up.

2. State of the art

2.1. Synergistic co-digestion of food waste and waste activated sludge

The co-digestion of food waste and waste activated sludge (WAS) has been identified as an effective strategy to overcome the limitations of mono-substrate fermentation. In our previous studies, we have also investigated this approach, confirming its potential to enhance process stability and overall performance [7, 8]. Food waste provides readily fermentable carbohydrates but is typically deficient in nitrogen, whereas WAS supplies protein, nutrients, and active microbial biomass [9]. Their combination improves the $\mathrm{C/N}$ ratio, enhances buffering capacity, and supports a more diverse microbial community, leading to improved hydrogen production and process stability.

Kora et al. [9] demonstrated that the addition of protein-rich co-substrates enhances buffering capacity, mitigates pH instability, and promotes more efficient substrate utilization, resulting in higher hydrogen yields compared to single-substrate systems. Furthermore, the use of WAS reduces the need for external inoculation and improves operational robustness, providing a practical advantage for large-scale applications. These combined effects form the basis for the co-digestion strategy adopted in this study.

2.2. Sequential integration of dark fermentation and anaerobic digestion

Studies on two-stage biological conversion systems further confirm the advantages of integrating dark fermentation and anaerobic digestion. Jung et al. [10] demonstrated that a two-stage dynamic membrane bioreactor treating food waste can achieve stable operation at organic loading rates up to 5.0 $\mathrm{g_{COD}/(L.d)}$, while maintaining efficient methane recovery. The system enabled recovery of up to 79% of the chemical energy contained in the substrate, highlighting the effectiveness of sequential hydrogen and methane production. Overall, the DF-AD cascade improves energy recovery, enhances substrate utilization, and contributes to stable reactor performance under varying operating conditions. A key requirement for effective integration is the removal of hydrogen from the dark fermentation effluent prior to anaerobic digestion. Gas-liquid separation prevents hydrogen consumption by methanogens and ensures proper separation between hydrogen and methane production pathways.

2.3. Process simulation of integrated biological systems using Aspen Plus

Aspen Plus is widely used for modeling complex biological waste-to-energy systems due to its ability to represent coupled reaction networks, phase behavior, and mass and energy balances within a unified framework [11]. The platform provides flexible reactor models that enable the implementation of kinetic and stoichiometric descriptions of dark fermentation and anaerobic digestion processes.

Anaya Menacho et al. [11] demonstrated the capability of Aspen Plus for modeling food waste anaerobic digestion, reporting methane contents of 74.82% and 77.10% at fat concentrations of 40% and 60%, respectively, under organic loading rates between 2 and 5 $\mathrm{L/day}$. The model was validated against experimental data with minimal variances (1.2% to 2.5%), confirming its reliability for predicting biogas composition. These results highlight the applicability of Aspen Plus as a tool for analyzing process performance under varying operating conditions.

2.4. Aim of the study

A critical review of the literature indicates that, while individual aspects of bioenergy production such as food waste fermentation, waste activated sludge treatment, and DF-AD integration have been widely studied, their combined representation within a unified and experimentally validated framework remains limited. In particular, the integration of heterogeneous feedstock characterization, kinetic modeling, and process simulation into a single consistent platform has not been fully addressed.

This study aims to develop and validate a mechanistically consistent Aspen Plus simulation framework for the integrated production of biohydrogen and biomethane from food waste and waste activated sludge using a sequential DFAD configuration. The model is validated against experimental data obtained from a 50 L semi-continuous dark fermentation reactor and demonstrates reliable prediction of the downstream anaerobic digestion stage.

A key contribution is the implementation of a Python-based feedstock characterization framework, which translates the compositional variability of food waste into simulation-ready inputs while ensuring elemental mass balance closure. The validated model provides a flexible platform for process optimization, energy performance evaluation, and future scale-up of integrated biological waste-to-energy systems.

3. System description and methodology

3.1. Overall system configuration

The integrated system is designed for energy recovery from a co-digestion substrate consisting of 12 kg of waste activated sludge and 3 kg of food waste. While the experimental campaign is conducted in a single physical reactor, the simulation framework adopts a mechanistic decoupling approach to account for the fundamentally different biochemical pathways and kinetics governing carbohydrate and protein degradation. The overall process flowsheet is presented in Figure. 1.

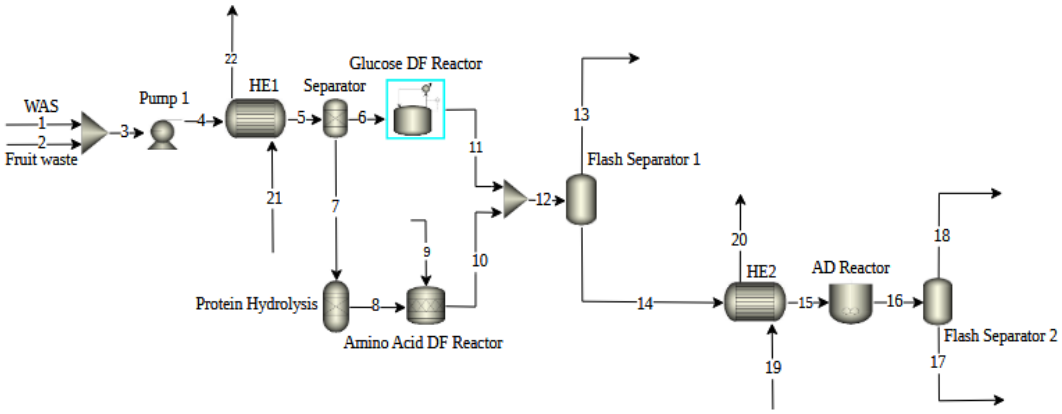

Figure. 1. Schematic flowsheet of the integrated dark fermentation and anaerobic digestion simulation in Aspen Plus.

Within the model, the feed is partitioned into carbohydrate-rich and protein-rich fractions to enable pathway-specific representation. The carbohydrate fraction is processed in a BATCHOP reactor, where dark fermentation is described through acetate- and butyrate-type pathways, incorporating time-dependent microbial growth, substrate consumption, and hydrogen partial pressure inhibition. In parallel, the protein fraction undergoes a two-stage conversion, consisting of non-kinetic hydrolysis in a RYIELD reactor followed by stoichiometric fermentation in an RSTOIC reactor, resulting in the formation of volatile fatty acids (VFAs), hydrogen, carbon dioxide, and ammonia.

The combined effluent from the dark fermentation stage is directed to a flash separator operating at near-atmospheric conditions, where the gaseous phase - primarily composed of hydrogen and carbon dioxide - is removed. This step prevents hydrogen consumption via hydrogenotrophic methanogenesis in the downstream anaerobic digestion unit, thereby preserving net hydrogen recovery. The remaining liquid phase, enriched in VFAs and residual soluble substrates, is subsequently heated to 52 °C to establish thermophilic conditions prior to anaerobic digestion. A final flash separation unit is used to recover methane-rich biogas and liquid digestate, ensuring consistent phase separation and closure of mass and energy balances across the integrated system.

3.2. Feedstock characterization and representation

The co-digestion substrate consists of waste activated sludge (WAS) and food waste. While WAS exhibits relatively stable physicochemical properties, food waste is characterized by significant compositional variability arising from seasonal availability and source-dependent factors, as reported in Table 1. This variability affects the distribution of key biochemical components and consequently influences fermentation pathways and hydrogen production performance. Furthermore, the elemental composition of waste activated sludge (WAS) was characterized using EPA report [12].

Table 1. Approximate composition of food waste used for mixture generation[12]

FOOD WASTE	CARBOHYDRATES (g)	PROTEINS (g)	LIPIDS (g)	ASH (g)	ORGANIC ACIDS (g)	SUGARS (g)	FIBERS (g)
APPLE	13.0	0.35	0.20	0.40	0.35	11.0	2.50
ONION	9.0	1.25	0.15	0.75	0.00	6.0	1.75
EGGPLANT	4.5	1.25	0.20	0.65	0.20	2.5	2.50
TOMATO	3.5	1.00	0.35	0.75	0.30	2.5	1.50
CITRUS	9.0	0.90	0.20	0.50	0.75	8.0	1.50
LETTUCE	2.5	0.75	0.15	0.40	0.15	1.5	1.50
FENNEL	4.5	1.25	0.20	0.90	0.20	3.5	2.50
ORANGE	12.0	0.90	0.20	0.50	0.80	9.0	2.40
KIWI	14.5	1.10	0.50	0.60	1.00	8.5	3.00
CELERY	3.0	0.70	0.20	0.60	0.10	1.5	1.60

To ensure compatibility with the deterministic requirements of Aspen Plus, a Python-based data processing framework was developed to generate simulation-ready feedstock representations. Food waste was described using surrogate biochemical components, including carbohydrates, proteins, lipids, and organic acids. For general modeling purposes, a probabilistic approach based on Monte Carlo sampling was implemented to capture compositional variability and derive statistically representative feed compositions. For experimental validation, predefined mixtures (Mix A+B and Mix C, as reported in Figure 2) were directly implemented. The framework was used to compute the corresponding elemental composition and ensure mass and elemental balance closure. The resulting compositions were introduced as deterministic inlet streams in Aspen Plus, enabling consistent integration of experimental data with the simulation model.

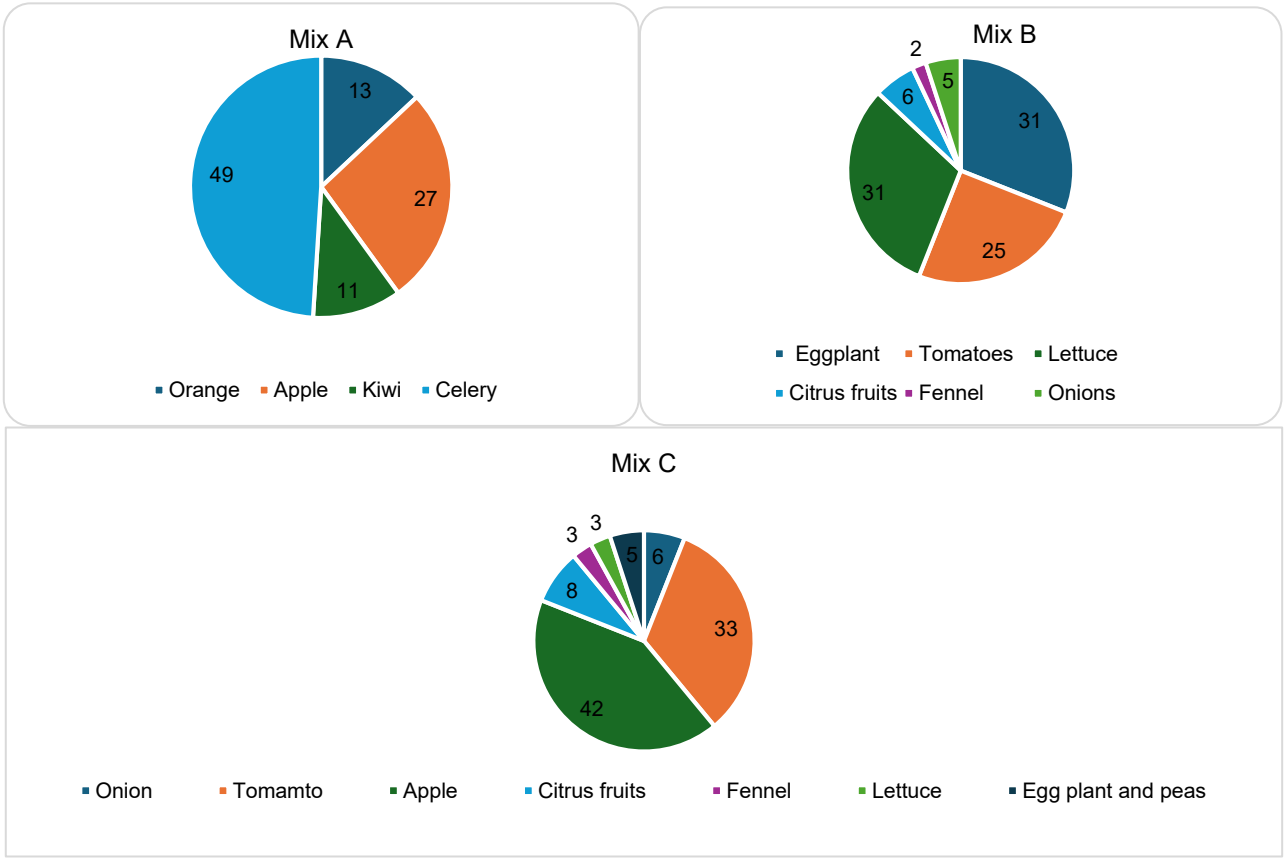

Figure. 2. Composition of food waste mixtures used in experimental and modeling analysis.

3.3. Dark fermentation reactor configuration

Due to the different biochemical pathways of carbohydrates and proteins, dark fermentation was modelled using two parallel routes. Glucose fermentation was implemented in an Aspen Plus BATCHOP reactor to capture time-dependent kinetics and hydrogen partial pressure effects. Protein degradation was represented as a two-step process: hydrolysis into amino acids using a RYIELD reactor based on literature distributions, followed by stoichiometric conversion in an RSTOIC reactor to produce VFAs, hydrogen, carbon dioxide, and ammonia.

3.3.1. Kinetic modelling of glucose dark fermentation

Glucose conversion during dark fermentation was modeled using a BATCHOP reactor in Aspen Plus. Experimental results indicated that acetic acid and butyric acid were the dominant soluble fermentation products, while other metabolites such as propionate, ethanol, and lactate were present in negligible concentrations. Accordingly, glucose fermentation was represented through two parallel metabolic pathways: an acetate-type pathway and a butyrate-type pathway. The acetate-type pathway corresponds to the classical hydrogen-producing stoichiometry:

$$C_6H_{12}O_6 + 2H_2O \rightarrow 2CH_3COOH + 2CO_2 + 4H_2, \quad (1)$$

whereas the butyrate-type pathway follows:

$$C_6H_{12}O_6 \rightarrow CH_3CH_2CH_2COOH + 2CO_2 + 2H_2, \quad (2)$$

The fermentation kinetics were implemented using the built-in biomass growth model in Aspen Plus, where glucose (S) is consumed by active biomass (X), represented by Clostridium. The general biomass growth rate is defined as:

$$\frac{dX}{dt} = \mu X, \quad (3)$$

where μ is the specific growth rate and X is the active biomass concentration.

Substrate consumption is linked to biomass growth through the true yield coefficient $Y_{s:x}$ and a maintenance term M_s:

$$\frac{dS}{dt} = -Y_{s:x}\frac{dX}{dt} - M_s X - \frac{\beta}{Y_{p:s}}X, \quad (4)$$

Where S is glucose concentration, $Y_{s:x}$ is true biomass yield on substrate, M_s is maintenance coefficient, β is non-growth-associated production coefficient, and $Y_{p:s}$ is product yield on substrate.

Product formation for each pathway (acetate and butyrate) follows a mixed growth-associated and non-growth-associated model:

$$\frac{dP}{dt} = Y_{p:x}\frac{dX}{dt} + \beta X, \quad (5)$$

Where $Y_{p:x}$ is product yield on biomass.

Two separate product definitions were implemented within the same BATCHOP reactor to represent the acetate and butyrate pathways, each with its own yield parameters consistent with experimental observations.

To account for thermodynamic and metabolic inhibition caused by hydrogen accumulation, an explicit hydrogen partial pressure inhibition function was introduced through a custom kinetic term. The inhibition factor was defined as:

$$I_{H_2} = \exp\left(\frac{P_{H_2}}{K_{H_2}}\right), \quad (6)$$

Where P_{H_2} is hydrogen partial pressure in the gas phase and, K_{H_2} is inhibition constant.

The effective specific growth rate becomes:

$$\mu_{eff} = \mu . I_{H_2}, \quad (7)$$

Thus, as hydrogen accumulates, the exponential term reduces the effective growth rate and consequently lowers substrate consumption and product formation rates. This formulation reproduces the experimentally observed sensitivity of dark fermentation to hydrogen backpressure and allows differentiation between semi-closed and gas-vented reactor configurations.

The dark fermentation reactor was modeled as a BATCHOP unit operating under mesophilic conditions at a fixed temperature of 34 °C. The reactor volume was specified as 50 L, and vapor-liquid phases were considered to account for gas production during fermentation. The system was operated under variable pressure conditions, with pressure calculated dynamically during the simulation. A semi-continuous operation strategy was implemented through pressure-controlled venting, where gas release occurs at a vent opening pressure of 1.2 bar and closes at 1 bar, ensuring controlled hydrogen removal. The initial reactor pressure was set to 1 bar, with nitrogen (N_2) used as an inert pad gas. The batch cycle included a feed time of 1 hour, a discharge time of 1 hour, and no downtime between cycles, with a total batch operation time of 24 hours. Reaction kinetics and mass transfer effects were included, while crystallization and catalytic effects were neglected.

3.3.2. Protein hydrolysis and amino acid fermentation

Protein hydrolysis was modelled using a RYIELD reactor, where the protein fraction of WAS decomposed into its constituent amino acids based on literature-reported distributions [13]. Subsequently, amino acid fermentation was simulated using an RSTOIC reactor, where stoichiometric reactions derived from established anaerobic pathways [14] were implemented to convert amino acids into volatile fatty acids, hydrogen, carbon dioxide, and ammonia. This approach provides an elementally consistent representation of protein-derived fermentation.

3.4. Gas-liquid separation and integration with downstream units

Following dark fermentation, the reactor effluent is directed to a flash unit operating at near-atmospheric conditions to achieve vapor-liquid equilibrium. The gas phase, primarily composed of hydrogen and carbon dioxide, is separated from the liquid phase, which contains volatile fatty acids (VFAs) and residual soluble substrates.

The separated gas stream is recovered as the hydrogen-rich product, while the liquid stream is routed to the anaerobic digestion (AD) unit for further conversion. This configuration ensures phase separation between gaseous and liquid products prior to downstream processing and enables independent operation of the subsequent AD stage.

3.5. Anaerobic digestion reactor modelling

The AD stage was modelled in Aspen Plus using a continuous stirred tank reactor (RCSTR). The reaction network and kinetic parameters were adopted from the literature [15] to represent the main biochemical pathways, including acidogenic, acetogenic, and methanogenic conversions. The model describes the transformation of soluble substrates such as VFAs and residual organics into methane, carbon dioxide, and water. Reaction rates were implemented using power-law kinetics based on reported rate constants, ensuring an elementally consistent representation of anaerobic digestion. The reactor was modelled under the following simplifying assumptions: perfect mixing, isothermal operation at 52 °C, constant pressure, and steady-state conditions. Inhibition effects related to pH and free ammonia were neglected.

Following anaerobic digestion, the reactor effluent is separated using a flash unit operating at near-atmospheric conditions. The vapor phase, mainly composed of methane and carbon dioxide, constitutes the produced biogas, while the liquid phase contains residual species and biomass. This separation step enables accurate quantification of methane production and prevents losses due to gas dissolution in the liquid phase.

4. Results and discussion

4.1. Feedstock characterization

The inlet feedstock composition is summarized in Table 2 and defined in Aspen Plus as the food waste input stream. Two configurations are considered: a combined mixture of 50% Mix A and 50% Mix B, and Mix C. In both cases, the composition is dominated by glucose, indicating that carbohydrate-based fermentation pathways are expected to govern the dark fermentation process.

A comparison between the two mixtures shows that Mix C contains a higher glucose fraction and slightly lower structural carbohydrate content (cellulose and hemicellulose) relative to Mix A+B. This shift in composition increases the availability of readily fermentable substrates, which is expected to enhance hydrogen production during the dark fermentation stage.

Table 2. Inlet stream composition (mass fraction) (50% Mix A + 50% Mix B and Mix C).

Component	**Mass Fraction**	
Mixture	Mix A+B	Mix C
Glucose	0.513	0.566
Cellulose	0.156	0.138
Hemicellulose	0.033	0.029
Lignin	0.033	0.029
Proteins	0.155	0.096
Linoleic acid	0.031	0.031
Ash	0.053	0.072
Citric acid	0.012	0.018
Acetic acid	0.012	0.018

4.2. Dark fermentation results

The performance of the dark fermentation stage was evaluated by comparing simulated liquid metabolites and gaseous outputs against reported experimental ranges and averages. As shown in Table 3, both simulated configurations (Mix A+B and Mix C) demonstrate high fidelity in reproducing the dominant metabolic pathways.

The predicted concentrations of acetic and butyric acids are in close agreement with experimental observations, confirming that the model accurately captures the acetate- and butyrate-type fermentation routes. Similarly, the simulated hydrogen production rate and gas composition fall within the reported experimental ranges, indicating a consistent representation of the biochemical conversion processes.

The comparison between Mix A+B and Mix C shows only minor variations in both liquid and gaseous products, suggesting that the system response is stable with respect to the change in feedstock composition. The slight increase in hydrogen production observed for Mix C can be attributed to its higher glucose content compared to Mix A+B, which enhances substrate availability for fermentative pathways and consequently leads to an increased hydrogen production rate.

Overall, the limited deviation from experimental data confirms the robustness and predictive capability of the implemented kinetic and stoichiometric framework under the selected operating conditions.

Table 3. Comparison of simulated and experimental dark fermentation outputs.

Parameter	**Unit**	**Simulation value**		**Experimental range**	**Exp. average**
		Mix A+B	Mix C		
Acetic acid	mM	10.21	10.3	4.8-29.0	10.2
Butyric acid	mM	8.46	8	0-13.4	8.9
HPR	$\mathrm{NLH_2/(L \cdot d)}$	0.79	0.8	0.7-0.83	-
Hydrogen per Glucose	$\mathrm{mol_{H_2}/mol_{Glucose}}$	1.54	1.54	1.45-2.5	-
H_2 molar fraction	$\mathrm{mol_{H_2}/mol_{tot}}$	0.51	0.52	0.4-0.6	-
CO_2 molar fraction	$\mathrm{mol_{CO_2}/mol_{tot}}$	0.49	0.48	0.4-0.5	-

4.3. Dynamic hydrogen production behaviour

The temporal evolution of hydrogen production is illustrated in Figure 3. Both configurations exhibit a characteristic dynamic profile, with an initial increase in hydrogen generation rate corresponding to the exponential microbial growth phase, followed by a peak and a subsequent decline due to hydrogen partial pressure inhibition. This behavior is consistent with experimental observations and reflects the underlying kinetics of dark fermentation.

After the peak, the hydrogen production rate decreases as hydrogen accumulates in the system, inhibiting further production. The application of intermittent gas removal mitigates this effect, leading to a stabilization of the production rate at later stages. This trend reflects the semi-continuous operational strategy adopted in the reactor, where pressure-controlled venting is used to limit hydrogen inhibition.

A clear distinction is observed between the two configurations, with Mix C consistently exhibiting higher hydrogen generation rates compared to Mix A+B throughout the process. This behavior is attributed to the higher glucose content in Mix C, which enhances substrate availability and promotes increased hydrogen production.

Overall, the model successfully captures the dynamic behavior of hydrogen production, including the growth phase, peak formation, inhibition effects, and subsequent stabilization. This confirms the capability of the implemented kinetic model to represent the interaction between microbial activity and hydrogen inhibition under the selected operating conditions.

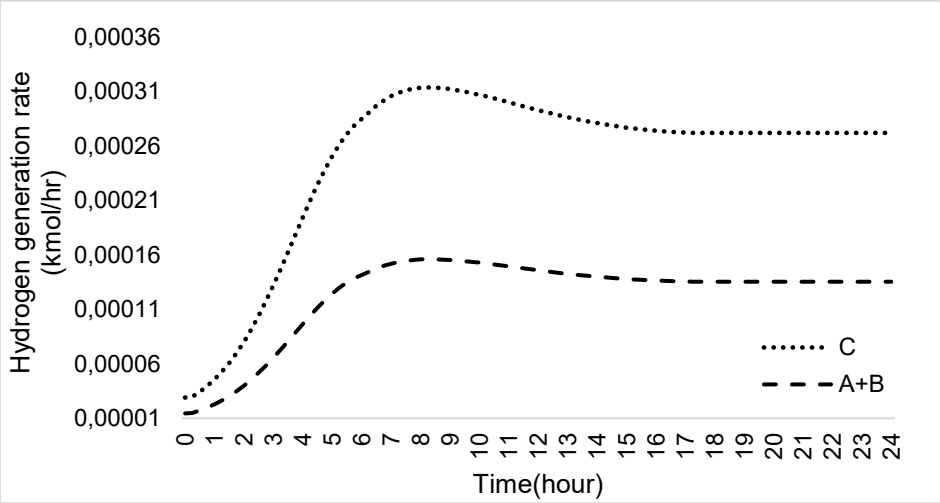

Figure. 3. Hydrogen generation rate.

4.4. Anaerobic digestion results

The simulation indicates near-complete conversion of the residual organic substrates within the anaerobic digestion stage, consistent with the thermophilic operating conditions. As summarized in Table 4, both Mix A+B and Mix C exhibit very high conversion of acetic acid, confirming that the model adequately represents the methanogenic pathways responsible for methane formation, with acetoclastic methanogenesis playing a dominant role under the considered conditions.

The simulated methane production rate and specific methane yield indicate effective conversion of fermentation intermediates into methane, suggesting that the anaerobic digestion stage operates without significant kinetic limitations under the selected conditions.

A comparison between the two configurations shows a moderate increase in methane production for Mix C. This behavior is attributed to the higher availability of biodegradable intermediates generated during the upstream dark fermentation stage, which leads to an increased substrate supply for methanogenesis.

Overall, the results support the validity of the implemented kinetic framework and demonstrate that the integrated DF-AD configuration enables stable and effective conversion of organic substrates into methane.

Table 4. Simulated anaerobic digestion performance indicators.

Parameter	Unit	Simulation value		Significance
		Mix A+B	Mix C	
Residual glucose conversion	%	99.9	99.88	Near-complete degradation
Acetic acid conversion	%	99.52	99.48	Primary methanogenic substrate
Methane production rate	$\mathrm{L/h}$	54.18	58.24	Primary energy output
Specific methane yield	$\mathrm{L/kg_{COD}}$	123.47	124.44	High-efficiency conversion

5. Conclusions

This study presents a mechanistically consistent and experimentally validated Aspen Plus simulation of an integrated dark fermentation and anaerobic digestion process for the co-conversion of food waste and waste activated sludge into biohydrogen and biomethane. The developed framework successfully captures the key biochemical pathways governing both hydrogen and methane production, demonstrating strong agreement with experimental observations.

The integration of dark fermentation and anaerobic digestion enables effective recovery of residual organic intermediates, significantly enhancing overall energy conversion efficiency. The thermophilic anaerobic digestion stage ensures high substrate utilization, confirming the suitability of the proposed configuration for maximizing energy recovery from heterogeneous waste streams.

A key contribution of this work is the implementation of a Python-based feedstock characterization approach, which enables consistent representation of variable organic substrates while ensuring elemental balance closure within the simulation environment. This feature enhances the robustness and applicability of the model for real-world waste-to-energy systems.

Overall, the validated simulation framework provides a reliable tool for process analysis, optimization, and scale-up of integrated biological conversion systems. It establishes a foundation for future studies on system integration, process intensification, and sustainable energy production from organic waste.

Acknowledgments

The research activity has been founded by MoDSEn project: “MODel of Saving electric ENergy from organic waste fermentation” CSEAB_00364, financed by Italian Minister of Economic Development, 20 September 2021, published on G.U.R.I. n.234, 30 September 2021.

Nomenclature

Latin symbols

K_{H_2} hydrogen partial pressure inhibition constant, Pa

M_s substrate maintenance coefficient, $\mathrm{g_{substrate}/(g_{biomass}.h)}$

P_{H_2} hydrogen partial pressure, Pa

S substrate concentration, $\mathrm{g/L}$

X active biomass concentration, $\mathrm{g/L}$

$Y_{p:x}$ growth-associated product yield coefficient, $\mathrm{g_{product}/g_{biomass}}$

$Y_{s:x}$ true biomass yield coefficient, $\mathrm{g_{substrate}/g_{biomass}}$

Greek symbols

β non-growth-associated production coefficient, $\mathrm{g_{product}}/(\mathrm{g_{biomass}}.\mathrm{h})$

μ specific growth rate, h^{-1}

μ_{eff} effective specific growth rate, h^{-1}

Abbreviations

AD anaerobic digestion

DF dark fermentation

FW food waste

HPR hydrogen production rate

NL normal liter

RCSTR continuous stirred tank reactor (Aspen Plus block)

SOFC solid oxide fuel cell

VFA volatile fatty acid

WAS waste activated sludge

References

[1] Khuyinrud MB, Kalan AS, Lü X, et al. Evaluating Solar Energy Potential for Power, Heat, and Green Hydrogen Production: Exergy and Dynamic Analysis Across Italy. 2026, pp. 216–227.

[2] Babaei Khuyinrud M, Shokri Kalan A, Pourtalebi B, et al. Design, performance assessment, and machine learning-driven optimization of a novel low-carbon urban waste-to-x polygeneration system: multi-scenario analysis of hydrogen and methane production. *Energy* 2026; 344: 140052.

[3] Martínez-Mendoza LJ, García-Depraect O, Muñoz R. Unlocking the high-rate continuous performance of fermentative hydrogen bioproduction from fruit and vegetable residues by modulating hydraulic retention time. *Bioresour Technol* 2023; 373: 128716.

[4] Martínez-Mendoza LJ, Lebrero R, Muñoz R, et al. Influence of key operational parameters on biohydrogen production from fruit and vegetable waste via lactate-driven dark fermentation. *Bioresour Technol* 2022; 364: 128070.

[5] Jung J-H, Sim Y-B, Ko J, et al. Biohydrogen and biomethane production from food waste using a two-stage dynamic membrane bioreactor (DMBR) system. *Bioresour Technol* 2022; 352: 127094.

[6] Anaya Menacho W, Mazid AM, Das N. Modelling and analysis for biogas production process simulation of food waste using Aspen Plus. *Fuel* 2022; 309: 122058.

[7] Linzi L, Stoppato A, Tassinato G, et al. TECHNOLOGIES AND ENERGY STRATEGIES FOR THE PRODUCTION AND UTILIZATION OF GREEN HYDROGEN IN THE INDUSTRIAL SECTOR. In: *37th International Conference on Efficiency, Cost, Optimization, Simulation and Environmental Impact of Energy Systems (ECOS 2024)*. Zografos, Greece: ECOS 2024, 2024, pp. 1303–1314.

[8] Linzi L, Stoppato A, Chinello D, et al. INTEGRATING DARK FERMENTATION AND SOFC TECHNOLOGY: OPTIMIZING BIOHYDROGEN UTILIZATION FOR GREEN ENERGY, https://www.research.unipd.it/handle/11577/3556953 (2025, accessed 17 April 2026).

[9] Kora E, Patrinou V, Antonopoulou G, et al. Dark fermentation of expired fruit juices for biohydrogen production followed by treatment and biotechnological exploitation of effluents towards bioplastics and microbial lipids. *Biochem Eng J* 2023; 195: 108901.

[10] Jung J-H, Sim Y-B, Ko J, et al. Biohydrogen and biomethane production from food waste using a two-stage dynamic membrane bioreactor (DMBR) system. *Bioresour Technol* 2022; 352: 127094.

[11] Anaya Menacho W, Mazid AM, Das N. Modelling and analysis for biogas production process simulation of food waste using Aspen Plus. *Fuel* 2022; 309: 122058.

[12] Tabella di composizione degli alimenti - CREA, https://www.crea.gov.it/-/tabella-di-composizione-degli-alimenti (accessed 17 April 2026).

[13] Zhang W, Alvarez-Gaitan JP, Dastyar W, et al. Value-Added Products Derived from Waste Activated Sludge: A Biorefinery Perspective. *Water (Basel)* 2018; 10: 545.

[14] Ramsay IR, Pullammanappallil PC. Protein degradation during anaerobic wastewater treatment: derivation of stoichiometry. *Biodegradation* 2001; 12: 247–256.

[15] Rajendran K, Kankanala HR, Lundin M, et al. A novel process simulation model (PSM) for anaerobic digestion using Aspen Plus. *Bioresour Technol* 2014; 168: 7–13.